

热分解法制备 $\text{Y}_2\text{O}_2\text{S}:\text{Eu}^{3+}$ 纳米粒子

谭宁会 王国媛 廖佩坤 刘艺成 孟建新 刘应亮*
(广州市暨南大学化学系暨南大学纳米化学研究所, 广州 510632)

摘要: 采用热分解法和硫熔法分别合成了纳米 $\text{Y}_2\text{O}_2\text{S}:\text{Eu}^{3+}$ 和体相 $\text{Y}_2\text{O}_2\text{S}:\text{Eu}^{3+}$ 。其中硫氧化钇纳米粒子的制备是以水热法合成的 $\text{Y}(\text{OH})_3$ 为前驱体, 随后在激活剂和硫的共同作用下焙烧得到的。结果表明, 所得 $\text{Y}_2\text{O}_2\text{S}:\text{Eu}^{3+}$ 为单一纯相纳米粒子, 粒径分布集中, 大小约 80 nm, 而前驱体 $\text{Y}(\text{OH})_3$ 为纳米棒状, 形貌上的这一巨大变化是由激活剂和硫粉在高温煅烧过程所形成的熔融物的腐蚀作用造成的。荧光光谱分析表明, Eu^{3+} 能有效地掺入硫氧化钇基质中, 并具有良好的发光性能。此外, 还探讨了纳米粒子的形成机理。

关键词: 硫氧化钇; 纳米粒子; 发光性能; 机理

中图分类号: O614.32

文献标识码: A

文章编号: 1001-486(2010)08-1421-05

Nanocrystals $\text{Y}_2\text{O}_2\text{S}:\text{Eu}^{3+}$ Prepared by Thermolysis

TAN Ning-Hui WANG Yuan-Yuan LIAO Pei-Kun LIU Yi-Cheng
MENG Jian-Xin LIU Ying-Liang*
(Department of Chemistry, Jinan University, Guangzhou 510632)

Abstract: This paper reports the preparation process of $\text{Y}_2\text{O}_2\text{S}:\text{Eu}^{3+}$ nano-crystals by thermolysis method and the corresponding bulk $\text{Y}_2\text{O}_2\text{S}:\text{Eu}^{3+}$ by conventional sulfur flux method. Nano-crystals $\text{Y}_2\text{O}_2\text{S}:\text{Eu}^{3+}$ were synthesised by calcining the rod-like $\text{Y}(\text{OH})_3$ precursor, obtained from hydrothermal method, with co-activator and S powder. The results show that both bulk and nano-crystals $\text{Y}_2\text{O}_2\text{S}:\text{Eu}^{3+}$ are with pure phase, hexagonal crystal structure. The hydrothermally prepared $\text{Y}(\text{OH})_3$ is in a rod-like morphology, while the calcined $\text{Y}_2\text{O}_2\text{S}:\text{Eu}^{3+}$ are narrow distributed nano-crystals, with an average size of 80 nm. The morphological change can be explained by the etching effect of the flux formed by the carbonate and S powder during high temperature calcination. It is concluded that Eu^{3+} could be effectively incorporated into yttrium oxysulfides and therefore shows good luminescent properties from the excitation and emission spectra. Besides, the mechanism is discussed too.

Key words: yttrium oxysulfide; nano-crystals; luminescent properties; mechanism

0 Introduction

Rare earth oxysulfide materials often exhibit high luminescence efficiency. These materials are widely used as luminescent host materials such as red emitting phosphors for color television picture tube and long

afterglow materials^[1]. Coarser particles of rare earth oxysulfide phosphors obtained from conventional high-temperature solid state reaction can not meet the requirements for higher resolution image rendering devices. The fabrication of $\text{Y}_2\text{O}_2\text{S}:\text{Eu}^{3+}$ nano-crystals has attracted much attention recently. Jagannathan et al

收稿日期: 2010-03-29。收修改稿日期: 2010-05-10。

国家自然科学基金(No.20671042), 广东省自然科学基金(No.0520055)资助项目。

*通讯联系人。E-mail: tliuyi@jnu.edu.cn, Fax: +86-20-85220597; 会员登记号: S060017521P。

第一作者: 谭宁会, 女, 25 岁, 硕士研究生; 研究方向: 纳米材料与环境材料。

synthesized nano-crystal $\text{Y}_2\text{O}_3\text{:Eu}^{3+}$ by two step sol-gel polymer thermolysis method^[2-6] and hydrothermal method^[7]. Pires et al^[8] prepared $\text{Y}_2\text{O}_3\text{:Yb}$ (4%), Er (0.1%) and $\text{Y}_2\text{O}_3\text{:Yb}$ (4%), Tm (0.1%) from polymeric and basic carbonate precursors. Besides, an ethanol assisted combustion synthesis method was adopted to prepare $\text{Y}_2\text{O}_3\text{:Eu}^{3+}$ nano-crystals by Luo et al^[1]. But the products are either seriously aggregated or still big in particle size. Although Fu et al^[9] obtained well-dispersed $\text{Y}_2\text{O}_3\text{:Eu}^{3+}$ nanocrystals with a combustion method by adding polyvinyl alcohol (PVA) to prevent the particles from agglomeration. The raw material CS (NH_2)₂ they used is toxic. The fabrication of nano-crystals $\text{Y}_2\text{O}_3\text{:Eu}^{3+}$ with small size remains a challenge. To the best of our knowledge, there has been no detail information on the growth mechanism of $\text{Y}_2\text{O}_3\text{:Eu}^{3+}$ nano-crystals.

In our previous work, long-lasting phosphorescent material $\text{Y}_2\text{O}_3\text{:Eu}^{3+}$, Ti^{4+} ^[10] and $\text{Y}_2\text{O}_3\text{:Eu}^{3+}$, Mg^{2+} , Ti^{4+} ^[11] were prepared by co-precipitation method and hydrothermal-microwave method, respectively. In this work, $\text{Y}_2\text{O}_3\text{:Eu}^{3+}$ nano-crystals were synthesized through hydrothermal method followed by subsequent thermal decomposition in presence of sulfur. The experimental results confirm that the $\text{Y}_2\text{O}_3\text{:Eu}^{3+}$ nano-crystals are narrow distributed small particles with an average size of 80 nm. The mechanism is discussed too.

1 Experimental

1.1 Synthesis of Eu^{3+} doped yttrium oxysulfide nano-crystals

The main starting materials were Y_2O_3 (99.99%), Eu_2O_3 (99.99%) and sulfur (A.R. grade). In a typical synthesis, Y_2O_3 was dissolved in nitric acid (65%) to get a clear solution and the pH value was adjusted to 12~13 by adding NaOH solution (5 mol · L⁻¹) under vigorous stirring. The mixture was then transferred to Teflon lined stainless autoclave and heated at 180 °C for 12 h. A white precipitate was collected, washed with distilled water and ethanol for several times, and dried in air at 60 °C. Then the as prepared $\text{Y}(\text{OH})_3$ nano-rod was mixed with certain amount of Eu_2O_3 , Na_2CO_3 and sulfur,

in which Y_2O_3 , S and Na_2CO_3 with a mass ratio of 10:3:3 while Y^{3+} and Eu^{3+} with a molar ratio of 1:0.03. The mixture was thoroughly mixture and ground then heated in muffle furnace at 850 °C for 5 h under carbon monoxide atmosphere. Then the products were dipped in dilute HCl (0.1 mol · L⁻¹) for about 1 h and washed with distilled water and ethanol for several times. For comparison, bulk $\text{Y}_2\text{O}_3\text{:Eu}^{3+}$ was synthesized by conventional sulfur flux method^[9].

1.1 Characterization

X-ray power diffraction (XRD) data of the products were collected at room temperature using MSAL-XRD2 automatic X-ray Diffractometer with Cu $K\alpha$ (40 kV, 20 mA, $\lambda = 0.154\,06\text{ nm}$) and a scanning rate of 8° · min⁻¹. Transmission electron microscopy (TEM) was used to detect the shape of the products, using an accelerating voltage of 100 kV. Samples for TEM were prepared by dropping a diluted suspension of the sample powders onto a standard carbon-coated film on a copper grid and air-dried. Photoluminescence measurements were performed on a Hitachi F-4500 Fluorescence spectrophotometer equipped with a 150 W xenon lamp as the excitation source at room temperature.

2 Results and discussion

2.1 Crystal structure and morphology of $\text{Y}(\text{OH})_3$ precursor

The XRD pattern of the precursor after hydrothermal route is shown in Fig.1. The well developed sharp diffraction peaks and flat baseline indicate good crystallinity of the powder. All the peaks can be indexed into hexagonal structure, and the

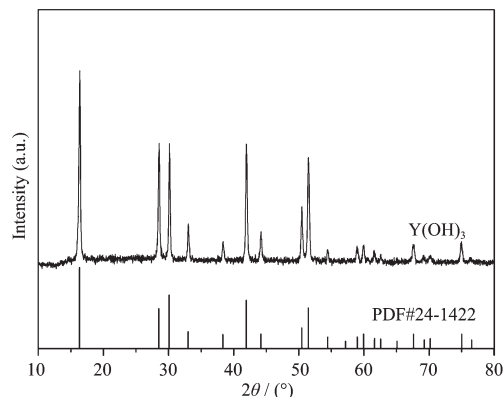


Fig.1 XRD patterns of $\text{Y}(\text{OH})_3$

lattice parameters are calculated from the pattern with $a=6.026$ nm and $c=3.544$ nm, in good agreement with the standard powder diffraction file, PDF#24-1422. No peaks attributable to other products are identified, suggesting that a pure phase of hexagonal $\text{Y}(\text{OH})_3$ powder is prepared by hydrothermal route.

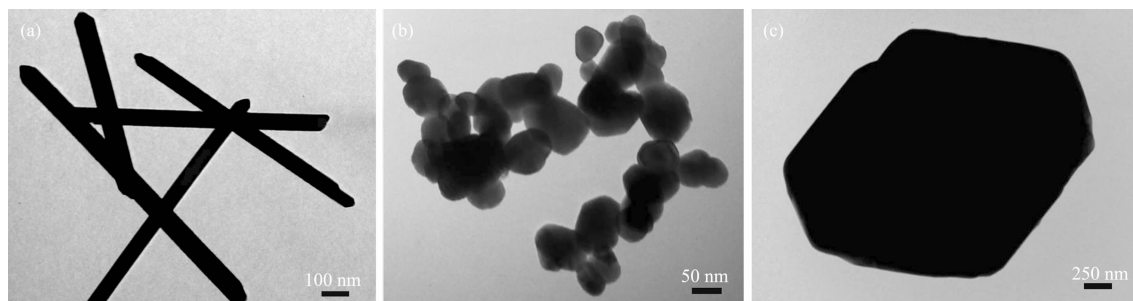


Fig.2 TEM images of $\text{Y}(\text{OH})_3$ (a), $\text{Y}_2\text{O}_3\text{:Eu}^{3+}$ nano-crystals(b) and bulk $\text{Y}_2\text{O}_3\text{:Eu}^{3+}$ (c)

2.2 Phase identification of $\text{Y}_2\text{O}_3\text{:Eu}^{3+}$

Fig.3 shows the XRD patterns of bulk and nanocrystalline $\text{Y}_2\text{O}_3\text{:Eu}^{3+}$. Both of the patterns for bulk and nanocrystalline $\text{Y}_2\text{O}_3\text{:Eu}^{3+}$ are different from the $\text{Y}(\text{OH})_3$ precursor shown in Fig.1, suggesting a new phase. Another hexagonal structure with lattice parameter a of 0.385 2 nm and c of 0.666 7 nm could be indexed from the pattern, which is in good consistence with the standard XRD data of Y_2O_3 (PDF #24-1424). No diffraction peaks attributable to other products are observed, indicating high purity of the products. Na_2CO_3 serves as co-activator and the byproducts are washed away completely. The XRD pattern shows sharp diffraction features in bulk $\text{Y}_2\text{O}_3\text{:Eu}^{3+}$ but much broader and less intense peaks in $\text{Y}_2\text{O}_3\text{:Eu}^{3+}$ nano-crystals because of their much smaller grain size and lower degree of crystallinity.

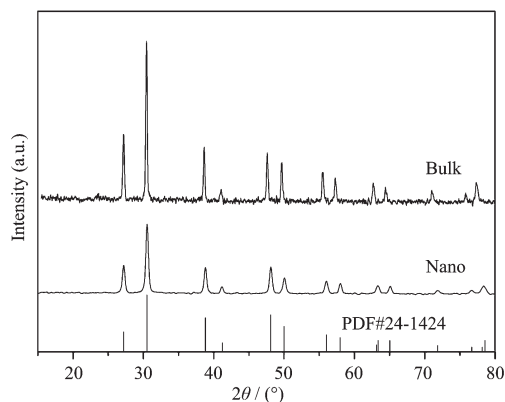


Fig.3 XRD patterns of $\text{Y}_2\text{O}_3\text{:Eu}^{3+}$

As can be seen from Fig.2a, $\text{Y}(\text{OH})_3$ powder with uniform shape and size is obtained by the hydrothermal method, showing the advantage of this method in preparing particles with uniform size. All the particles show rod-like shape, and the diameter is 70~80 nm.

2.3 Morphology and growth mechanism of $\text{Y}_2\text{O}_3\text{:Eu}^{3+}$ nano-crystals

Transmission electron microscope images of nano-crystalline and bulk $\text{Y}_2\text{O}_3\text{:Eu}^{3+}$ are shown in Fig.2(b,c). As estimated from the TEM micrograph, the diameter of the bulk $\text{Y}_2\text{O}_3\text{:Eu}^{3+}$ prepared by conventional method are several microns while the diameter of $\text{Y}_2\text{O}_3\text{:Eu}^{3+}$ nanocrystals prepared by hydrothermal method are 70~80 nm, corresponding to the size of the precursor $\text{Y}(\text{OH})_3$. However, in this case, quite different from our expectance, the rod-like structure of the precursor $\text{Y}(\text{OH})_3$ is broken, and uniform particles are obtained. This indicates a tremendous shape change from the precursor to the product. This may result from the unstability of the precursor $\text{Y}(\text{OH})_3$ or the etching effect of the flux formed by the alkali carbonates and sulfur powder during the calcination. Perhaps both factors are functioning synergistically.

Further experiments reveal that the shape change from the precursor to the product is attributed to the etching effect of the flux. If the precursor is heated alone without the flux at 850 °C or higher for 5 h, the Y_2O_3 obtained is nano-rod too (Fig.4b), indicating that the shape change is not caused by the decomposition of the precursor. If the mixture is heated at lower temperature, rod-like morphology of the precursor is partly preserved. The morphology of the final product in this case is neither rod-like nor nano-particles, but rod-

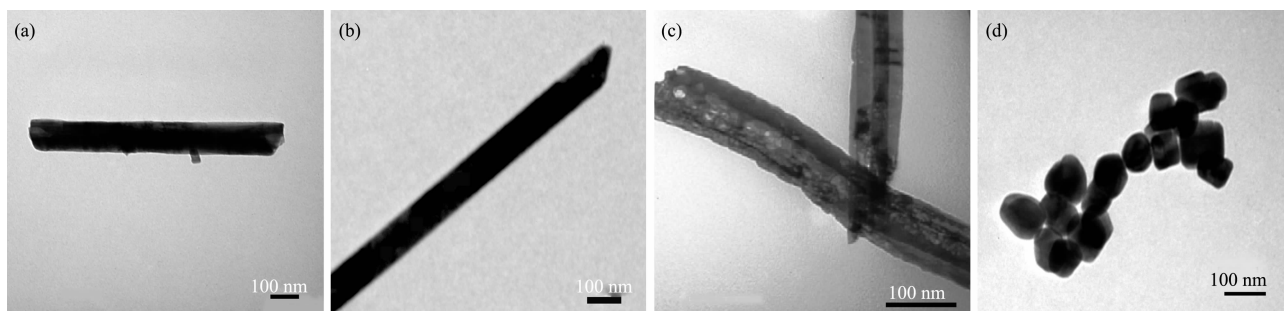
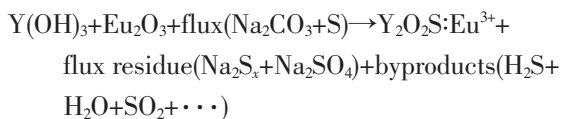


Fig.4 TEM images of Y(OH)₃(a), Y₂O₃(b), 800 °C 2 h for intermediate(c) and Y₂O₂S:Eu³⁺(d)

like with some crevasses(Fig.4c). Therefore we suggest that the flux of Na₂CO₃ and sulfur corrupt the precursor^[9]. The thermolysis reaction proceeds as follows:



The flux corrupts the precursor Y(OH)₃ and then crevasses are formed. As time passes, rod-like structure is broken, nano-particles are formed. When the products are dipped in dilute HCl, flux residue is dissolved. All the byproducts are washed away by distilled water and anhydrous ethanol, only Y₂O₂S:Eu³⁺ nano-particles are left. This result is in accordance with the XRD and TEM analysis. No impurity phases are detected, and the particles are well-dispersed(Fig. 4d). According to the literature^[12], different flux will produce oxysulfide with different shapes. A scheme for the formation of spherical particles is illustrated in Fig.5.

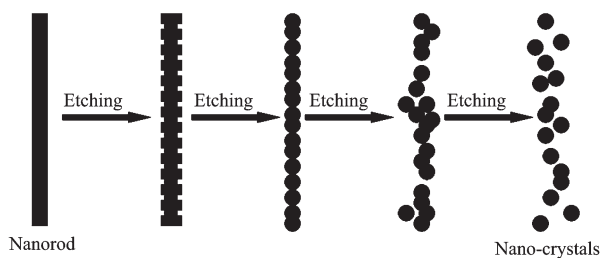


Fig.5 A scheme for a nanorod to nano-crystals conversion by the etching of alkali melt during the calcination

2.4 Luminescent spectra analysis

The excitation spectrum was performed by monitoring the emission of Eu³⁺ ⁵D₀ → ⁷F₂ transition at 626 nm. There are two charge transfer(CT) bands in the

excitation spectra for Y₂O₂S:Eu³⁺ from Fig.6a, the one around 280 nm attributes for S²⁻ → Eu³⁺ while the other around 346 nm attributes for O²⁻ → Eu³⁺^[6]. The emission intensities caused by O²⁻ → Eu³⁺ are much stronger than S²⁻ → Eu³⁺. Upon excitation at 314 nm, the emission spectra of the products are obtained (Fig.6b). The strong red-emission lines at 626 nm and 614 nm are due to the transition from ⁵D₀ → ⁷F₂ level of Eu³⁺ and its strongest peak is at 626 nm. Other transition from the ⁵D_J(J=0, 1) excited levels to ⁷F_J(J=0, 1, 2, 3, 4, 5, 6) ground states are very weak. Both the excitation peaks and the emission peaks are almost the same in position for bulk

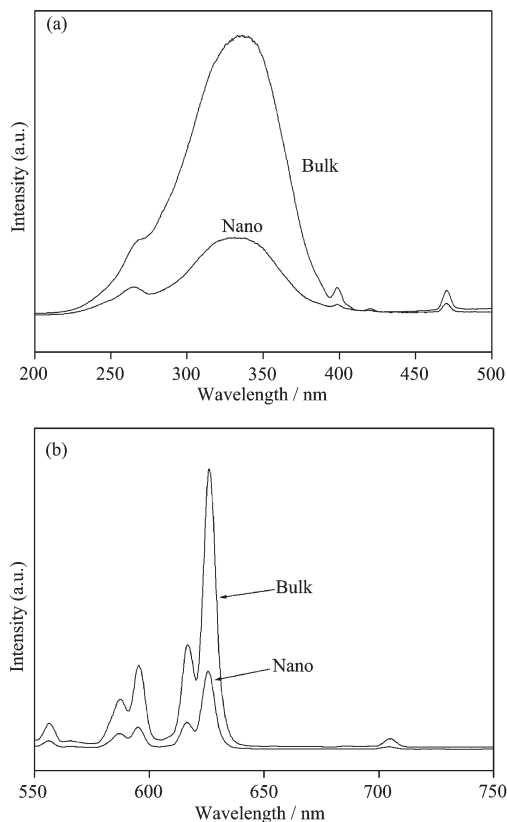


Fig.6 (a)Excitation and (b) emission spectra of Y₂O₂S:Eu³⁺

and nanocrystalline $\text{Y}_2\text{O}_2\text{S}:\text{Eu}^{3+}$ but all the peaks of nanocrystalline $\text{Y}_2\text{O}_2\text{S}:\text{Eu}^{3+}$ are much less intense than the uncoated $\text{Y}_2\text{O}_2\text{S}:\text{Eu}^{3+}$, which may result from the great demission of the particle size.

3 Conclusions

In summary, well-dispersed $\text{Y}_2\text{O}_2\text{S}:\text{Eu}^{3+}$ nanocrystals were synthesized through hydrothermal method followed by thermal decomposition in presence of sulfur. The results indicate that both bulk and nanocrystals $\text{Y}_2\text{O}_2\text{S}:\text{Eu}^{3+}$ are in pure phase, hexagonal crystal structure. The hydrothermally prepared $\text{Y}(\text{OH})_3$ reveals a rod-like morphology, while the calcined $\text{Y}_2\text{O}_2\text{S}:\text{Eu}^{3+}$ are narrow distributed nano-crystals about 80 nm. The morphological change can be explained by the etching effect of the melt formed by the carbonate and S powder during the high temperature calcination. It is therefore concluded that Eu^{3+} could be effectively incorporated into yttrium oxysulfides, resulting in good luminescent properties from the excitation and emission spectra. Besides, the mechanism is discussed too. Hydrothermal method offers a very simple way of fabricating well-crystallized nano-crystals.

References:

- [1] Luo X X, Cao W H, Xing M M. *J. Rare Earths*, **2006**,**24**:20-24
- [2] Dhanaraj J, Jagannathan R, Trivedi D C. *J. Mater. Chem.*, **2003**,**13**:1778-1782
- [3] Dhanaraj J, Geethalakshmi M, Jagannathan R, et al. *Chem. Phys. Lett.*, **2004**,**387**:23-28
- [4] Thirumalai J, Jagannathan R, Trivedi D C. *J. Lumin.*, **2007**, **126**:353-358
- [5] Nakkiran A, Thirumalai J, Jagannathan R. *Chem. Phys. Lett.*, **2007**,**436**:155-161
- [6] Thirumalai J, Chandramohan R, Sekar M, et al. *J. Nanopart. Res.*, **2008**,**10**:455-463
- [7] Thirumalai J, Chandramohan R, Auluck S, et al. *J. Colloid Interface Sci.*, **2009**,**336**:889-897
- [8] Pires A M, Serra O A, Davolos M R. *J. Alloys Compd.*, **2004**,**374**(1/2):181-184
- [9] Fu Z L, Geng Y, Chen H W, et al. *Opt. Mater.*, **2008**,**31**:58-62
- [10] HE Gan-Wu(贺干武), LIU Ying-Liang(刘应亮), ZHANG Jun-Wen(张俊文). *Chinese J. Inorg. Chem. (Wuji Huaxue Xuebao)*, **2007**,**23**(2):315-318
- [11] LI Wen-Yu(李文宇), LIU Ying-Liang(刘应亮), AI Peng-Fei(艾鹏飞). *Chinese J. Inorg. Chem. (Wuji Huaxue Xuebao)*, **2008**,**24**(5):772-776
- [12] Hang T, Liu Q, Mao D L, et al. *Mater. Chem. Phys.*, **2008**, **107**:142-147